Melanocortin 4 receptors in autonomic neurons regulate thermogenesis and glycemia

Published in final edited form as:
Nat Neurosci. 2014 July ; 17(7): 911–913. doi:10.1038/nn.3737.

Melanocortin 4 receptors in autonomic neurons regulate thermogenesis and glycemia

Eric D. Berglund[1,*], **Tiemin Liu**[*], **Xingxing Kong**[2,*], **Jong-Woo Sohn**[3], **Linh Vong**[2], **Zhuo Deng**[4], **Charlotte E. Lee**[1], **Syann Lee**[1], **Kevin W. Williams**[1], **David P. Olson**[5], **Philipp E. Scherer**[6], **Bradford B. Lowell**[2,#], and **Joel K. Elmquist**[1,7,#]

[1]Division of Hypothalamic Research, Department of Internal Medicine, UT Southwestern Medical Center, Dallas, TX, 75390, USA

[2]Division of Endocrinology, Beth Israel Deaconess Medical Center and Harvard Medical School, Harvard University, Boston, MA, 02115, USA

[3]Department of Biological Sciences, Korea Advanced Institute of Science and Technology, Daejeon, 305-701, Korea

[4]Department of Obstetrics and Gynecology, The First Affiliated Hospital, Medical School of Xi'an Jiaotong University, Xi'an 710061, P.R. China

[5]Division of Endocrinology, Department of Pediatrics, University of Michigan, Ann Arbor, Michigan 48105, USA

[6]Touchstone Diabetes Center, Department of Internal Medicine, UT Southwestern Medical Center, Dallas TX, 75390, USA

[7]Department of Pharmacology, UT Southwestern Medical Center, Dallas TX, 75390, USA

SUMMARY

Melanocortin 4 receptors (Mc4rs) are expressed by extra-hypothalamic neurons including cholinergic autonomic pre-ganglionic neurons. However, whether Mc4rs in these neurons are required to control energy and glucose homeostasis is unclear. Here we report that *Mc4r*s in sympathetic, but not parasympathetic, pre-ganglionic neurons are required to regulate energy expenditure and body weight including brown and white adipose tissue thermogenic responses to diet and cold exposure. In addition, deletion of *Mc4rs* in both sympathetic and parasympathetic cholinergic neurons impairs glucose homeostasis.

[#]Co-corresponding Authors: Joel K. Elmquist, UT Southwestern/Room Y6.322, 5323 Harry Hines Blvd, Dallas, TX 75390-9077, joel.elmquist@utsouthwestern.edu. Bradford B. Lowell, Center for Life Sciences, Rm-703, 3 Blackfan Circle, Boston, MA 02115, blowell@bidmc.harvard.edu.
[*]Co-first authors

Author Contributions

E.D.B., T.L., and X.K. are co-first authors. E.D.B. designed and performed all experiments except gene expression and immunoblotting, analyzed the data, and wrote the manuscript. T.L. designed and performed all experiments except gene expression and immunoblotting, analyzed the data, and edited the manuscript. X.K. analyzed gene expression in adipose depots, performed immunoblotting in BAT, analyzed the data, and reviewed the manuscript. L.V. and D.P.O. designed and developed the *Mc4r*$^{flox/flox}$ mouse. D.P.O. designed and developed the *Chat-cre* mouse. K.W.W. and J.S. performed electrophysiological experiments. Z.D. and C.E.L. assisted performing experiments. P.E.S. designed experiments and edited the manuscript. B.B.L. and J.K.E. are both corresponding authors that supervised development of the mouse models, designed experiments, and edited the manuscript.

Distinct sub-sets of melanocortin 4 receptors (MC4Rs) in the CNS are established to exert segregated effects on tissues and processes underlying energy balance, glucose homeostasis, and cardiovascular function[1–5]. Notably, MC4Rs expressed outside the hypothalamus in pre-ganglionic cholinergic neurons of the sympathetic and parasympathetic nervous system have emerged as potential regulatory sites[3–5], thus raising the possibility that these sub-populations are crucial to control energy and glucose homeostasis. Extension of these and other data[6–9] further suggests that MC4Rs in sympathetic pre-ganglionic neurons may be required to stimulate thermogenesis in brown and white adipose tissue depots (BAT and WAT, respectively). This is noteworthy since thermogenic properties of BAT and WAT have recently become avid areas of interest to treat obesity and diabetes. However, the central pathway(s) that govern these processes are not fully understood.

To study requirement(s) for MC4Rs in the autonomic nervous system (ANS) to modulate energy and glucose homeostasis including role(s) of BAT and WAT depots, we generated genetically modified mice selectively lacking *Mc4r*s in pre-ganglionic autonomic neurons. Recently described *Mc4r*$^{flox/flox}$ mice[4] and animals expressing *cre*-recombinase (*cre*) in choline acetyltransferase positive neurons (*Chat-cre*[3]) were used to target sympathetic and parasympathetic pre-ganglionic neurons. Breeding *Mc4r*$^{flox/flox}$ and *Mc4r*$^{flox/flox}$ x *Chat-cre* mice produced expected progeny as well as littermates completely lacking *Mc4r* (*Mc4r*-null) due to early developmental expression of *cre*. Mice lacking *Mc4r*s in *Phox2B*-positive neurons[10] were used to assess MC4R function in autonomic control neurons including the dorsal motor nucleus of the vagus. Importantly, *Phox2b* is not expressed in sympathetic pre-ganglionic neurons. *In situ* hybridization and electrophysiological techniques similar to those used to confirm *Mc4r*$^{flox/flox}$ x *Chat-cre*[3, 4] mice show successful ablation of *Mc4r* in the dorsal motor nucleus of the vagus (DMV; Supplementary Figures 1A and 1B) that does not impair normal biophysical properties yet renders cells functionally insensitive to MC4R agonism (Supplementary Figures 1C–1F).

Since MC4R loss-of-function causes obesity in humans[1, 11, 12] and animals[1, 12], our first goal was to assess body weight. Chow-fed *Mc4r*$^{flox/flox}$ x *Chat-cre* mice initially exhibited normal body weight, but diverged at eight weeks-of-age and were ~ 40% heavier at 20 weeks-of-age (Figure 1A). This obesity was intermediate versus *Mc4r*-nulls and due to higher lean and fat mass (Figures 1A and 1B). It was also noted that body length was normal in *Mc4r*$^{flox/flox}$ x *Chat-cre* mice whereas *Mc4r*-null snout-to-anus distance was longer (data not shown). This is, to our knowledge, the first MC4R mutation causing obesity that is not confounded by altered growth. Metabolic cages were then used in young mice [to minimize differences in body weight (Figure 1A)] to isolate that *Mc4r*$^{flox/flox}$ x *Chat-cre* mice were obese due to low EE, not hyperphagia (Figures 1C–1D). As expected, global *Mc4r*-null mice were hypometabolic and hyperphagic (Figures 1C–1D). In contrast, chow-fed *Mc4r*$^{flox/flox}$ x *Phox2B-cre* revealed no differences in body weight or body composition (Supplementary Figures 2A–2B). Collectively, these results indicate that *Mc4r* signaling in cholinergic neurons, including sympathetic pre-ganglionic neurons, are required to maintain normal EE and thus body weight. *Mc4r*s in *Phox2b* neurons including those in the DMV, however, are dispensable for normal body weight homeostasis.

In addition to established roles of *Mc4r*s to control energy balance, growing evidence identifies role(s) to directly regulate glycemia. In agreement with this literature, we found that circulating glucose, insulin, and glucagon were elevated in young, body weight-matched, post-absorptive *Mc4r*$^{flox/flox}$ x *Chat-cre* mice similarly to *Mc4r*-null littermates (Figures 2A–2C). Only plasma insulin was elevated in *Mc4r*$^{flox/flox}$ x *Phox2B-cre* mice (Supplementary Figures 3A–3C). Intraperitoneal glucose tolerance tests further identified exaggerated glucose excursions and augmented plasma insulin responses in both groups suggestive of insulin resistance (Supplementary Figures 3D–3G). Hyperinsulinemic-euglycemic clamps in which blood glucose levels were matched in all groups during comparable increments in circulating insulin (Supplementary Figures 3H–3K) confirm this defect based on higher exogenous glucose infusion rates in both group (GIR; Figures 2D and 2E). Combined impairments in insulin-mediated suppression of endogenous glucose production (endoR_a) and stimulation of glucose disposal (R_d) were found to underlie lower GIR in *Mc4r*$^{flox/flox}$ x *Chat-cre* mice (Figures 2F). Additional analyses further identified that defects in iBAT, inguinal WAT (iWAT), and skeletal muscle (gastrocnemius and soleus) glucose uptake contribute to reduced R_d in *Mc4r*$^{flox/flox}$ x *Chat-cre* mice (Figure 2G). In contrast, impaired insulin-stimulated suppression of endoR_a is the sole contributor to reduced GIR in *Mc4r*$^{flox/flox}$ x *Phox2B-cre* mice (Figure 2H). These data demonstrate that *Mc4r*$^{flox/flox}$ x *Chat-cre* exhibit gluco-regulatory defects including hyperglycemia, hyperinsulinemia, hepatic insulin resistance, and hyperglucagonemia that in many respects are similar to *Mc4r*-null mice. *Mc4r*$^{flox/flox}$ x *Phox2B-cre* mice exhibit modest insulin resistance, but not overt hyperglycemia likely due to hyperinsulinemia. Collectively, these results demonstrate that *Mc4r* signaling in autonomic pre-ganglionic neurons are required to regulate glucose metabolism and insulin sensitivity.

We next challenged energy homeostasis in both *Mc4r*$^{flox/flox}$ x *Chat-cre* and *Mc4r*$^{flox/flox}$ x *Phox2B-cre* cohorts using high-fat/high-sucrose (HFHS) diet-induced obesity. Prior work has shown that whole-body *Mc4r*-deficient mice are more sensitive to diet-induced obesity[6, 7, 13]. Time-course analyses in *Mc4r*$^{flox/flox}$ x *Chat-cre* mice show that HFHS diet accelerated weight-gain resulting in obesity nearly comparable to *Mc4r*-null littermates (Figure 3A). Results from a metabolic cage paradigm similar to prior work[6] where HFHS diet is introduced to naïve, young (to minimize differences in body weight) chow-fed adult mice pinpoints that both hyperphagia and failure to fully increase EE likely underlies obesity in *Mc4r*$^{flox/flox}$ x *Chat-cre* mice (Figures 3B and 3C). Notably, these responses were similar to *Mc4r*-null littermates (Figures 3B and 3C) which are the predicted responses based on with prior work in other *Mc4r*-deficient mice fed an obesigenic diet[6, 7, 13]. Consistent with chow-fed data in *Mc4r*$^{flox/flox}$ x *Phox2B-cre* mice (see Supplementary Figure 2A), HFHS diet did not alter long-term body weight control in *Mc4r*$^{flox/flox}$ x *Phox2B-cre* mice or energy balance based on acute responses in metabolic cages (Supplementary Figures 4A–4C). Together, these data indicate that loss of extra-hypothalamic *Mc4r*s in cholinergic neurons including sympathetic pre-ganglionic neurons regulates diet-induced thermogenesis in contexts of an obesigenic diet.

Several studies have also suggested that *Mc4r* expressing neurons regulate intrascapular BAT (iBAT), which is potently regulated by the sympathetic nervous system and a key

component of adaptive thermogenesis[6–9]. We found that transcripts associated with heat production, fatty acid oxidation, and mitochondrial functions were reduced in chow-fed *Mc4r*$^{flox/flox}$ x *Chat-cre* iBAT (Supplementary Figure 4D). This was not the case in chow-fed *Mc4r*$^{flox/flox}$ x *Phox2B-cre* mice (Supplementary Figure 4E). Remote biotelemetry probes were next used to assess body temperature at 23°C and in response to cold (5 days at 6°C). These results show that basal body temperature was not reduced in *Mc4r*$^{flox/flox}$ x *Chat-cre* (Figure 3D). However, *Mc4r*$^{flox/flox}$ x *Chat-cre* mice were unable to engage adaptive thermogenesis and body temperature in cold-exposed *Mc4r*$^{flox/flox}$ x *Chat-cre* mice declined rapidly to *Mc4r*-null values within 4 h (Figure 3D). Analyses of iBAT histology and uncoupling protein 1 (UCP1) protein content after 120 h at 6°C further confirmed impaired thermogenic responses in *Mc4r*$^{flox/flox}$ x *Chat-cre* mice on par with defects in *Mc4r*-null littermates (Figure 3E and 3F). In addition, inguinal WAT (iWAT) in cold-exposed *Mc4r*$^{flox/flox}$ x *Chat-cre* mice failed to show evidence of “browning” based on gene expression (Supplementary Figure 4F) or histology for UCP1 (Figure 3G). Together, these data suggest that *Mc4r*s in sympathetic pre-ganglionic neurons are essential for adaptive thermogenesis including recruitment of iBAT and browning of iWAT. Notably, *Mc4r*s directly in these neurons are also required to maintain body temperature following cold exposure.

These current studies extend and confirm conclusions that MC4Rs in both parasympathetic and sympathetic pre-ganglionic neurons are sufficient and required to maintain aspects of normal energy and glucose homeostasis[3]. Specifically, selective loss of *Mc4r* in the sympathetic pre-ganglionic neurons deleteriously and independently impacts both processes while deletion in the vagal motor neurons results in hyperinsulinemia and modest insulin resistance. Our evidence also demonstrates that *Mc4r*s in sympathetic pre-ganglionic neurons are required for diet- and cold-induced thermogenesis in iBAT and “browning” of iWAT. These are topical findings because existence of functional depots of iBAT in adult humans[14–18] and the ability of WAT[19, 20] to exhibit thermogenic properties characteristic of BAT are recently described findings. However, it is important to clarify that our data cannot firmly establish that defects in iBAT and/or ability to “brown” iWAT contribute to low EE and/or hyperglycemia in mice lacking *Mc4rs* in sympathetic pre-ganglionic neurons. Nonetheless, synthesis of these data with the existing literature connecting specific sub-populations of *Mc4r*s to specific tissues and processes shows that SNS-mediated mechanisms regulate an array of tissues including the pancreas, liver, BAT, and WAT. In contrast, *Mc4r*-mediated control via the DMV appears restricted to pancreatic beta cells and circulating insulin. Outlining these functional connections is potentially important to develop more selective strategies to target *Mc4r*s or related pathways. Caution is warranted, however, as targeting *Mc4r*s to stimulate iBAT, browning of iWAT, or other EE mechanisms to exert beneficial effects in contexts of obesity and/or diabetes may cause sympathetic nervous system side effects. We propose that these extra-hypothalamic *Mc4r*s underlie key defects associated with melanocortin 4 receptor mutations in humans and that these sites are critical components involved in coordinated control of energy and glucose homeostasis.

Methods

Animal Care

Mc4r$^{flox/flox}$, *Chat-cre*, and *Phox2B-cre* mice on a C57BL/6J background have been previously described[3, 4]. Mice were group housed (1–5 mice per cage) in a barrier facility at 23°C unless otherwise noted. Mice were provided Harlan Teklad 2016 chow diet and water *ad libitum* unless otherwise noted. High-fat/high-sucrose (HFHS; Research Diets D12331) diet, if applicable, was removed and refilled weekly. Mice losing >10% of body weight during the acclimation period for metabolic cage studies (see below) or post-surgery prior to clamp studies (see below) were not studied. Body composition was measured using NMR (Bruker Mini-Spec).

Hormone Measurements

All measurements were done in duplicate. Insulin was measured using a commercial ELISA kit (Crystal Chem.). Glucagon was measured via RIA at the Vanderbilt University MMPC.

Metabolic Cages

Experiments were performed in a temperature-controlled room containing 36 TSE metabolic cages maintained by UTSW Animal Resources personnel. One week prior to study, mice were singly housed to acclimate to new housing. Three days prior to study, mice were transported to room containing metabolic cages to acclimate to a new environment. HFHS diet, if applicable, was also introduced at the beginning of this acclimation period. After 3 d acclimation, cages were connected to TSE system for a total of 5 d. Days 2–4 were used for data analyses.

Cold Exposure

Body temperature was assessed using biotelemetry probes (IPTT-300, BioMedic Data Systems) injected under anesthesia one-week prior. Mice were housed in cold chambers maintained at 6°C by UTSW Animal Resources personnel.

Clamp Studies

Experiments were done with the assistance of the UTSW Mouse Phenotyping Core.

Protein Extraction and Western Blot Analysis

Protein was extracted from BAT by using RIPA buffer (Boston BioProducts) supplemented with complete protease inhibitor cocktail (Roche). For western blot analyses, 60 mg protein was subjected to SDS-PAGE under reducing conditions, transferred, and blotted with the anti-UCP1 antibody (Abcam, ab10983).

Histology

Tissues were dissected and fixed in formalin for 48 h at 4°C followed by 50% ethanol. BAT histology was performed with assistance from the UTSW Histology Core. Inguinal white adipose tissue was performed with assistance from the Harvard Histology Core.

Analysis of Gene Expression by Quantitative PCR

Total RNA was extracted from tissues with TRIzol reagent (Invitrogen) according to the manufacturer's instructions. 1 μg total RNA was converted into first-strand cDNA with oligo(dT) primers as described by the manufacturer (Clontech). PCR was performed in an Mx3000P Q-PCR system (Stratagene) with specific primers and SYBR Green PCR Master Mix (Stratagene). The relative abundance of mRNAs was standardized with 36B4 mRNA as the invariant control.

Statistics

Sample sizes were determined using prior experience and power calculations designed to detect $p<0.05$ with a 15% variance. There were no methods to randomize mice to experimental groups. There were also no methods to blind investigators to genotype during experiments. Pre-established criteria for excluding data points were data two standard deviations outside the mean or any data obtained from mice that died or lost > 10% of body weight due to metabolic cage acclimation or clamp studies.

Supplementary Material

Refer to Web version on PubMed Central for supplementary material.

Acknowledgments

We thank Dr. Evan Rosen (Beth Israel Deaconess Medical Center and Harvard Medical School) for advice, assistance, and expertise. We also thank personnel in the UT Southwestern Mouse Phenotyping and Histology Cores as well as the NIH - Vanderbilt University Mouse Metabolic Phenotyping Core (MMPC) Hormone Assay and Analytical Core that is supported by DK 059637. This work was supported by NIH F32 DK092083 and K01 DK098317 awarded to E.D.B.; a mentor-based postdoctoral fellowship from the American Diabetes Association (7-11-MN-16) awarded to T.L.; a post-doctoral fellowship from American Heart Association (13POST16710016) awarded to X. Kong; NIH K01 DK087780 awarded to K.W.W.; a post-doctoral fellowship from the American Heart Association (12POST8860007) to J. Sohn; NIH R01 DK55758 and R01 DK099110 awarded to P.E.S as well as P01 DK088761 awarded to P.E.S. and J.K.E.; NIH R01 DK089044, R01 DK071051, R01 DK075632, R37 DK053477, and BNORC & BADERC Transgenic Core Grants P30DK046200 and P30DK057521 awarded to B.B.L.; and NIH R01 DK088423 and R37 DK053301 awarded to J.K.E.

References

1. Balthasar N, et al. Divergence of melanocortin pathways in the control of food intake and energy expenditure. Cell. 2005; 123:493–505. [PubMed: 16269339]
2. do Carmo JM, da Silva AA, Rushing JS, Pace B, Hall JE. Differential control of metabolic and cardiovascular functions by melanocortin-4 receptors in proopiomelanocortin neurons. American journal of physiology. Regulatory, integrative and comparative physiology. 2013; 305:R359–368.
3. Rossi J, et al. Melanocortin-4 receptors expressed by cholinergic neurons regulate energy balance and glucose homeostasis. Cell metabolism. 2011; 13:195–204. [PubMed: 21284986]
4. Sohn JW, et al. Melanocortin 4 receptors reciprocally regulate sympathetic and parasympathetic preganglionic neurons. Cell. 2013; 152:612–619. [PubMed: 23374353]
5. Zechner JF, et al. Weight-independent effects of roux-en-Y gastric bypass on glucose homeostasis via melanocortin-4 receptors in mice and humans. Gastroenterology. 2013; 144:580–590 e587. [PubMed: 23159449]
6. Butler AA, et al. Melanocortin-4 receptor is required for acute homeostatic responses to increased dietary fat. Nature neuroscience. 2001; 4:605–611.
7. Voss-Andreae A, et al. Role of the central melanocortin circuitry in adaptive thermogenesis of brown adipose tissue. Endocrinology. 2007; 148:1550–1560. [PubMed: 17194736]

8. Vaughan CH, Shrestha YB, Bartness TJ. Characterization of a novel melanocortin receptor-containing node in the SNS outflow circuitry to brown adipose tissue involved in thermogenesis. Brain research. 2011; 1411:17–27. [PubMed: 21802070]
9. Satoh N, et al. Satiety effect and sympathetic activation of leptin are mediated by hypothalamic melanocortin system. Neurosci Lett. 1998; 249:107–110. [PubMed: 9682828]
10. Pattyn A, Morin X, Cremer H, Goridis C, Brunet JF. Expression and interactions of the two closely related homeobox genes Phox2a and Phox2b during neurogenesis. Development. 1997; 124:4065–4075. [PubMed: 9374403]
11. Farooqi IS, et al. Clinical spectrum of obesity and mutations in the melanocortin 4 receptor gene. The New England journal of medicine. 2003; 348:1085–1095. [PubMed: 12646665]
12. Huszar D, et al. Targeted disruption of the melanocortin-4 receptor results in obesity in mice. Cell. 1997; 88:131–141. [PubMed: 9019399]
13. Srisai D, et al. Characterization of the hyperphagic response to dietary fat in the MC4R knockout mouse. Endocrinology. 2011; 152:890–902. [PubMed: 21239438]
14. Cypess AM, et al. Identification and importance of brown adipose tissue in adult humans. N Engl J Med. 2009; 360:1509–1517. [PubMed: 19357406]
15. Mirbolooki MR, Constantinescu CC, Pan ML, Mukherjee J. Quantitative assessment of brown adipose tissue metabolic activity and volume using 18F-FDG PET/CT and beta3-adrenergic receptor activation. EJNMMI research. 2011; 1:30. [PubMed: 22214183]
16. Virtanen KA, et al. Functional brown adipose tissue in healthy adults. N Engl J Med. 2009; 360:1518–1525. [PubMed: 19357407]
17. von Heydebreck A, Huber W, Poustka A, Vingron M. Identifying splits with clear separation: a new class discovery method for gene expression data. Bioinformatics. 2001; 17 (Suppl 1):S107–114. [PubMed: 11472999]
18. Orava J, et al. Different metabolic responses of human brown adipose tissue to activation by cold and insulin. Cell Metab. 2011; 14:272–279. [PubMed: 21803297]
19. Wu J, Cohen P, Spiegelman BM. Adaptive thermogenesis in adipocytes: is beige the new brown? Genes & development. 2013; 27:234–250. [PubMed: 23388824]
20. Tseng YH, Cypess AM, Kahn CR. Cellular bioenergetics as a target for obesity therapy. Nat Rev Drug Discov. 2010; 9:465–482. [PubMed: 20514071]

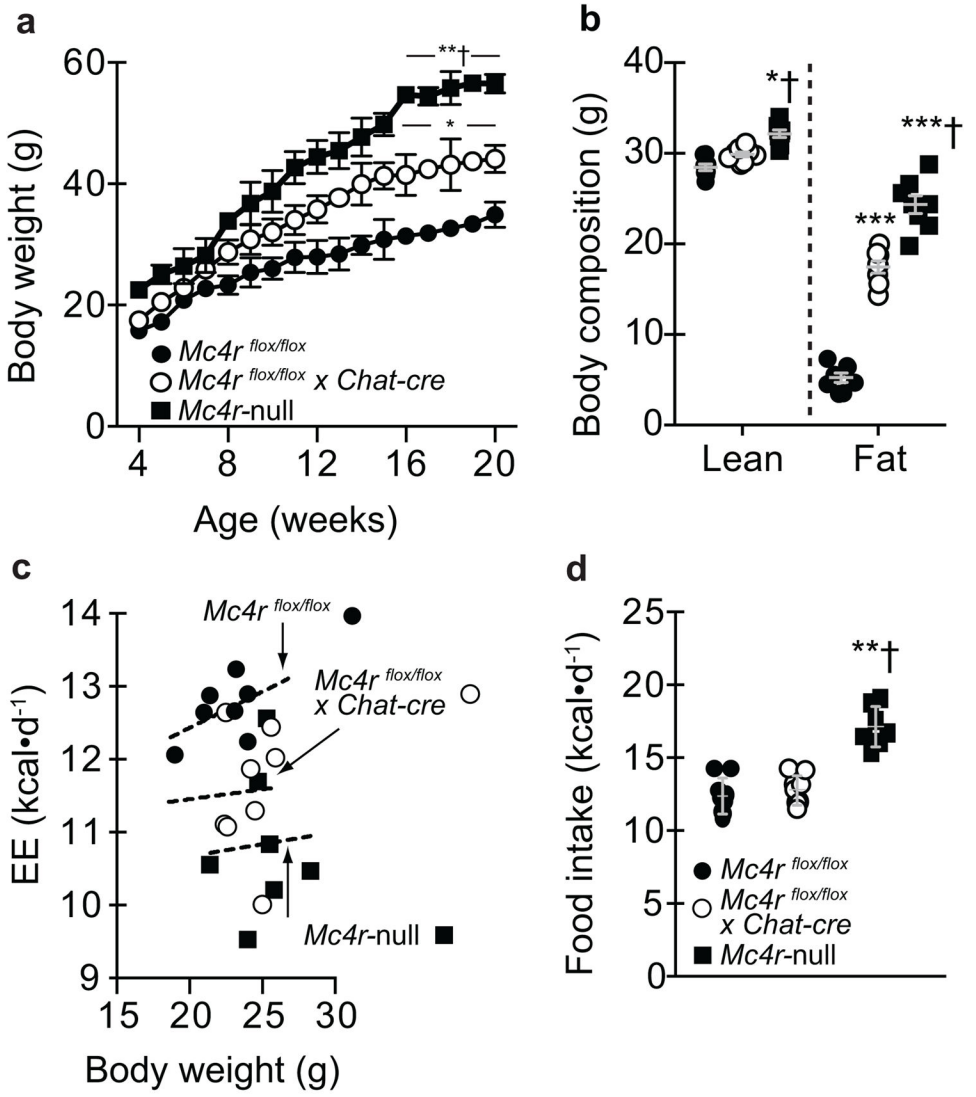

Figure 1.

Deleting melanocortin 4 receptors (*Mc4r*s) in pre-ganglionic cholinergic neurons in the sympathetic nervous system causes obesity due to reduced energy expenditure (EE). (a) Body weight in chow-fed mice with intact *Mc4r* signaling (controls; $Mc4r^{flox/flox}$), selective deletion of *Mc4r*s in cholinergic pre-ganglionic neurons ($Mc4r^{flox/flox}$x *Chat-cre*), or ectopic ablation of *Mc4r*s (*Mc4r*-null) (n = 10, 12, and 9, respectively). * and ** indicate $p<0.05$ or 0.01 versus $Mc4r^{flox/flox}$ mice and † indicates $p<0.05$ versus $Mc4r^{flox/flox}$x *Chat-cre* mice at indicated ages using one-way ANOVA followed by Tukey's post-hoc analyses. (b) Body composition in chow-fed 20 week-old $Mc4r^{flox/flox}$, $Mc4r^{flox/flox}$x *Chat-cre, and Mc4r*-null (n = 8, 8, and 7, respectively) littermate mice using NMR. * and *** indicate $p<0.05$ or 0.001 versus $Mc4r^{flox/flox}$ mice and † indicates $p<0.05$ versus $Mc4r^{flox/flox}$x *Chat-cre* mice at indicated ages using one-way ANOVA followed by Tukey's post-hoc analyses. (c) Energy expenditure (EE) and (d) food intake (EE) in 7- to 8-week-old chow-fed $Mc4r^{flox/flox}$, $Mc4r^{flox/flox}$ x *Chat-cre*, and *Mc4r*-null littermate mice (n = 9, 9, and 7,

respectively) over 5 d in TSE Metabolic Cages. Dashed lines in panel c denote linear regression of EE versus body weight in 7- to 8- week-old chow-fed male mice using ANCOVA. ** and † indicate in panel d indicate $p<0.01$ versus *Mc4r*$^{flox/flox}$ or *Mc4r*$^{flox/flox}$x *Chat-cre* mice, respectively, at indicated ages using one-way ANOVA followed by Tukey's post-hoc analyses. All mice were male and results are means ± SEM.

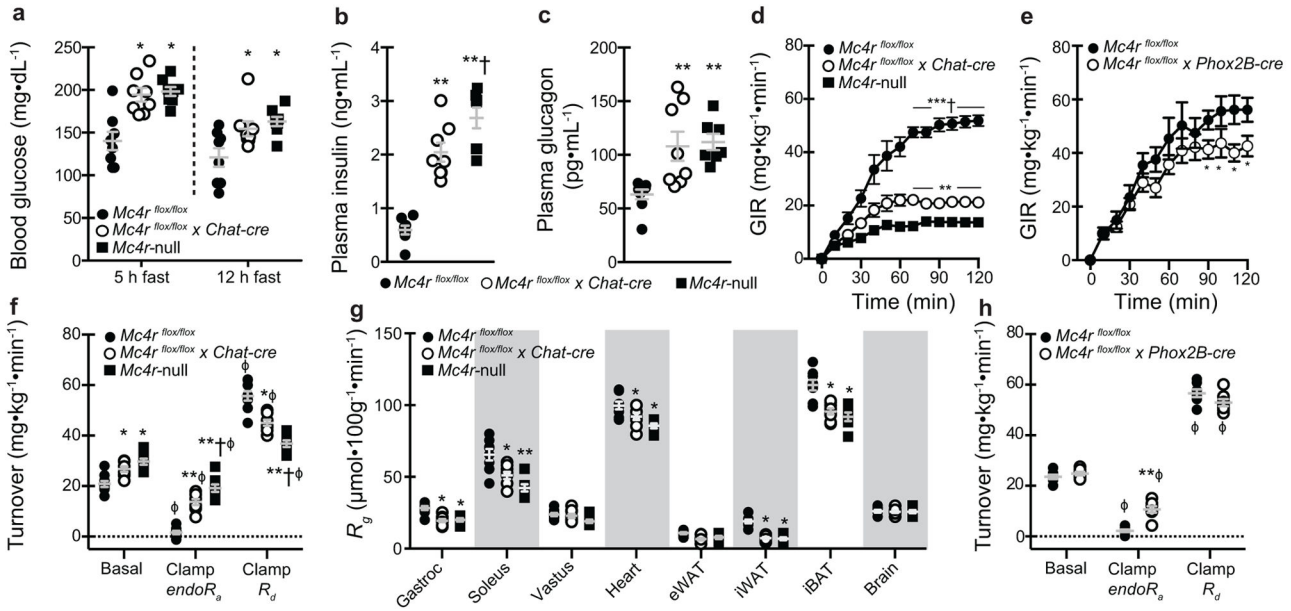

Figure 2.

Selective deletion of melanocortin 4 receptors (*Mc4r*s) in pre-ganglionic cholinergic neurons in the sympathetic nervous system cause gluco-regulatory abnormalities. (a) 5 h and 12 h fasted blood glucose, (b) 5 h fasted plasma insulin, and (c) 5 h fasted plasma glucagon in chow-fed mice with intact *Mc4r* signaling (*Mc4r*$^{flox/flox}$), selective deletion of *Mc4r*s in cholinergic pre-ganglionic neurons (*Mc4r*$^{flox/flox}$ x *Chat-cre*), and ectopic ablation of *Mc4r*s (*Mc4r*-null) (n = 8, 8, and 7, respectively). * and ** indicate p<0.05 or 0.01 versus *Mc4r*$^{flox/flox}$ mice and † indicates p<0.05 versus *Mc4r*$^{flox/flox}$ x *Chat-cre* mice using one-way ANOVA followed by Tukey's post-hoc analyses. (d) Exogenous glucose infusion rate (GIR) during hyperinsulinemic (4 mU/kg/min)-euglycemic clamps needed to maintain target glycemia of 150 mg/dL in *Mc4r*$^{flox/flox}$, *Mc4r*$^{flox/flox}$ x *Chat-cre*, and *Mc4r*-null littermate mice (n = 8, 8, and 7, respectively). *, **, and *** indicate p<0.05, 0.01, or 0.001, respectively, versus *Mc4r*$^{flox/flox}$ mice and † indicates p<0.001 versus *Mc4r*$^{flox/flox}$x *Chat-cre* mice at indicated times using one-way ANOVA followed by Tukey's post-hoc analyses. (e) GIR data in an independent cohort of *Mc4r*$^{flox/flox}$ and littermates lacking *Mc4r*s in the parasympathetic nervous system (*Mc4r*$^{flox/flox}$x *Phox2B-cre;* n = 7 and 8, respectively). * indicates p<0.05 versus *Mc4r*$^{flox/flox}$ using two-way repeat-measures ANOVA. (f) Basal and insulin-mediated changes in endogenous rate of glucose production (*endo*R_a) and disposal (R_d) during the clamp steady-state (t = 80–120 min). * and ** indicate p<0.05 or 0.01 versus *Mc4r*$^{flox/flox}$ mice and † indicates p<0.05 versus *Mc4r*$^{flox/flox}$ x *Chat-cre* mice using one-way ANOVA followed by Tukey's post-hoc analyses.. φ indicates p<0.05 comparing basal versus clamp within genotype using two-tailed paired Student's t-tests. (g) Tissue-specific glucose uptake (R_g) assessed during clamp steady-state (n = 8, 8, and 7, respectively). * and ** indicate p<0.05 or 0.01 versus *Mc4r*$^{flox/flox}$ mice using one-way ANOVA followed by Tukey's post-hoc analyses. (h) Basal and insulin-stimulated changes in *endo*R_a and R_d in *Mc4r*$^{flox/flox}$ and *Mc4r*$^{flox/flox}$ x *Phox2B-cre* mice (n = 7 and 6, respectively). * and ** indicate p<0.05 or 0.01 versus *Mc4r*$^{flox/flox}$ mice and † indicates p<0.05 versus *Mc4r*$^{flox/flox}$ x *Chat-cre* mice using two-tailed unpaired Student's t-tests. φ indicates p<0.05 comparing

basal versus clamp within genotype using two-tailed paired Student’s t-tests. All mice were male and results are means ± SEM.

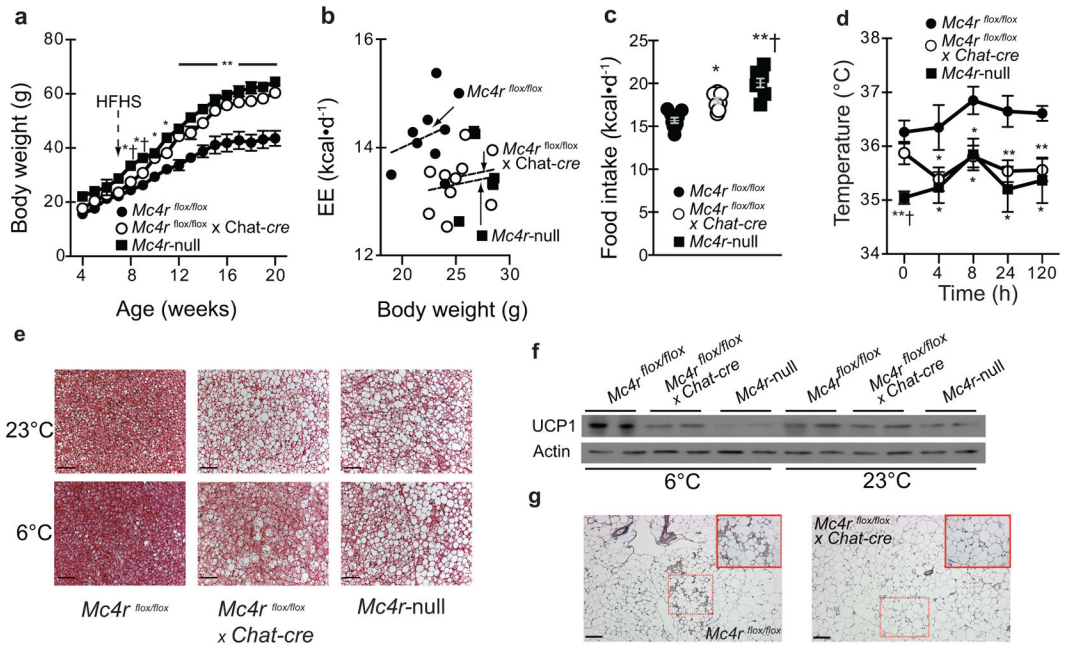

Figure 3.

Deletion melanocortin 4 receptors (*Mc4r*s) in pre-ganglionic cholinergic neurons promotes obesity as well as impairs BAT function and cold-tolerance. (a) Body weight in mice with intact *Mc4r* signaling (*Mc4r*$^{flox/flox}$), selective deletion of *Mc4r*s in cholinergic pre-ganglionic neurons (*Mc4r*$^{flox/flox}$ x *Chat-cre*), or ectopic ablation of *Mc4r*s (*Mc4r*-null) fed high-fat/high-sucrose (HFHS) after 8 weeks-of-age (n = 9, 12, and 9, respectively). * and ** indicate p<0.05 or 0.01 versus *Mc4r*$^{flox/flox}$ mice and † indicates p<0.05 versus *Mc4r*$^{flox/flox}$x *Chat-cre* mice using one-way ANOVA followed by Tukey's post-hoc analyses. (b) Energy expenditure (EE) and (c) food intake in chow-fed 7- to 8-week-old mice introduced to HFHS diet 3 d prior to metabolic cage assessment (n = 9, 10, and 7, respectively). Dashed lines in panel b denote linear regression of EE versus body weight in 7- to 8- week-old chow-fed male mice using ANCOVA. * and ** in panel C indicate p<0.05 or 0.01 versus *Mc4r*$^{flox/flox}$ mice and † indicates p<0.05 versus *Mc4r*$^{flox/flox}$ x *Chat-cre* mice using one-way ANOVA followed by Tukey's post-hoc analyses. (d) Basal (23°C) and cold (6°C)-induced body temperature determined by remote telemetry in chow-fed *Mc4r*$^{flox/flox}$, *Mc4r*$^{flox/flox}$ x *Chat-cre*, and *Mc4r*-null littermate mice (n = 8, 9, and 7, respectively) over 5 d. * and ** indicate p<0.05 or 0.01 versus *Mc4r*$^{flox/flox}$ mice and † indicates p<0.05 versus *Mc4r*$^{flox/flox}$ x *Chat-cre* mice using one-way ANOVA followed by Tukey's post-hoc analyses.(e) Representative images of iBAT histology as well as (f) UCP1 protein content. (g) Representative iWAT UCP1 staining (brown) in chow-fed *Mc4r*$^{flox/flox}$ and *Mc4r*$^{flox/flox}$ x *Chat-cre* littermate mice after 5 d cold exposure (n = 6 per genotype; inset upper right shows higher magnification of area outlined by dashed lines). Scale bars in panel e and g denote 50 and 100 uM, respectively. Full blots are shown in Supplementary Figure 5. Cold exposure experiments were repeated twice with success and there were no evident limitations in repeatability. All mice were male and results are means ± SEM.